

Research Paper

Construction of a human monoclonal antibody against bFGF for suppression of NSCLC

Sheng Wang^{1*}, Yiyang Qin^{1*}, Zhongmin Wang³, Junjian Xiang¹, Yu Zhang¹, Meng Xu², Baiyong Li³, Yu Xia³, Peng Zhang³, Hong Wang¹✉

1. Guangdong Province Engineering Research Center for antibody drug and immunoassay, College of Life Science and Technology, Jinan University, Guangzhou 510632, Guangdong Province, China.
2. Department of Oncology, the First Affiliated Hospital of Jinan University, Guangzhou 510632, Guangdong Province, China.
3. Akeso Biopharma, Inc., Zhongshan, 528400, Guangdong Province, China

* These authors contributed equally to this work.

✉ Corresponding author: Hong Wang; E-mail: wanghong368@yahoo.com; Tel: 008613602455251

© Ivyspring International Publisher. This is an open access article distributed under the terms of the Creative Commons Attribution (CC BY-NC) license (<https://creativecommons.org/licenses/by-nc/4.0/>). See <http://ivyspring.com/terms> for full terms and conditions.

Received: 2017.12.07; Accepted: 2018.02.13; Published: 2018.04.30

Abstract

Compelling evidence implicates that overexpression of basic fibroblast growth factor (bFGF) and fibroblast growth factor receptor 1 (FGFR1) in non-small cell lung cancer (NSCLC) drives tumor progression, can serve as prognostic biomarkers or therapeutic targets for NSCLC patients. But at present, we still lack of effective drugs for bFGF. The preparation of monoclonal antibodies against bFGF or to understand its mechanism of action is urgently need. Previously, we used hybridoma technology to produce a murine anti-bFGF monoclonal antibody (E12). However, E12 carries risks of heterogeneity and immunogenicity. In the present work, we produced three humanized variants (H1L1, H2L2 and H3L3) based on E12 by substituting residues in or near the complementarity-determining region (CDR). In addition, we thoroughly explored VH/VL domain combinations to simulate full-length IgG1 antibodies using computational protein design. H3L3 was selected for further study, as it demonstrated the best humanization and strongest affinity for bFGF. Specially, humanization of H3L3's light chain and heavy chain were 100% and 98.89%, respectively. The FGF2 neutralizing effect of H3L3 were confirmed by ELISA. We also found that H3L3 can effectively suppress the growth and angiogenesis of cancer through reduce the phosphorylation of AKT and MAPK. Moreover, H3L3 dramatically reduced tumor size and micro-vessel density in nude mice. Altogether, our study demonstrates that H3L3 exerts anti-tumor effects by impeding NSCLC development.

Key words: bFGF; Antibody humanization; Non-Small Cell Lung; Targeted therapies

Introduction

Lung cancer is among the most common cancers in the world with high morbidity and mortality rates. Specifically, non-small cell lung cancer (NSCLC) comprises 85% of all lung cancers and has a 5-year survival rate of only 4% in cases of metastatic disease[1]. Although current cancer treatments such as chemotherapy, radiotherapy and immunotherapy can improve overall survival (OS) and progression-free survival (PFS), only a subgroup of patients respond to these therapies. Compounding the problem, tumors are often not detected until they

have progressed to an advanced stage. However, angiogenesis or vascular remodeling is a major process of tumor cell metastasis and proliferation. Angiogenesis is a complex procedure involving several cell types. The maturation of endothelial cells to capillary tubes is a critical step[2, 3] and is the basis of forming a tumor-associated vascular network. Cancer cells utilize such angiogenic mechanisms to stimulate tumor growth. Stromal cells or tumor cells can secrete growth factors or chemokines that promote formation of blood vessels or lymph vessels.

Thus, finding effective targets to suppress angiogenesis for NSCLC treatment is urgently needed.

bFGF is a member of the FGF family. It is a cationic polypeptide of 155 amino acids that is highly conserved, associated with the angiogenesis or matrix remodeling in cancers[4]. bFGF interacts with the high-affinity FGFR and the low-affinity paran sulfate proteoglycans(HSPGs) [5]. Binding of bFGF to FGFRs induces a conformational change resulting in dimerization[6]and activation of the receptors' intracellular tyrosine kinase domains and downstream signaling pathways producing different pathological responses[7]. Moreover, dysregulation of FGF/FGFRs signaling in cancers contributes to pathogenesis[8]. Accumulating evidence has revealed that expression of bFGF and FGFRs is significantly elevated in the sera of multiple tumor types[9-11] and is associated with tumor recurrence[12]. bFGF and FGFR1 expression is commonly aberrant in early-stage NSCLC, and is associated with tumor growth, invasion, metastasis, and angiogenesis[13-16]. Thus, targeting bFGF /FGFRs may be an effective way to inhibit formation of blood vessels in tumors.

Several bFGF/FGFRs inhibitors have shown promising anti-angiogenic activity. Both monoclonal antibodies and tyrosine kinase inhibitors (TKIs) have been developed to target FGF2/FGFRs signaling networks[17-19]. Although FGFR TKIs, such as BIBF1120 and BMS-582, can block receptor signaling through competitive inhibition of ATP binding with the cytoplasmic domain of EGFR, FGFR and VEGFR, their low specificity and various side effects put a brake on clinical treatment. We attempted to prepare monoclonal antibodies to block the interaction between bFGF and FGFR1, to affect cell proliferation and angiogenesis. To this end, we previously produced an anti-bFGF murine monoclonal antibody (E12) by hybridoma technology, that showed promising antitumor activity[20, 21]. However, E12 would cause a potent anti-murine antibody response in humans. Therefore, it is necessary to humanize the antibody before conducting detailed pre-clinical and clinical studies. We have developed three novel human mAb against bFGF (H1L1, H2L2 and H3L3) based on E12 with computational protein design methods. We found that H3L3 can bind to bFGF specifically and displayed better humanization than the others. In addition, H3L3 could effectively target bFGF, weaken the interaction between bFGF and FGFR1, and prevent activation of downstream signal pathways. These activities exerted a strong antitumor activity in vitro and in vivo. Therefore, our study reveals that H3L3 is a promising candidate to inhibit the invasion, proliferation, migration, and angiogenesis of NSCLC.

Materials and methods

Cell culture and animals

Human lung cancer cells (H460) and human umbilical vein endothelial cells (HUVEC) were grown in DMEM (Gibco) media supplemented with 10% fetal bovine serum (Gibco) and 1% penicillin/streptomycin at 37°C in a 95% humidity atmosphere containing 5% CO₂.

BALB/c-nu mice (female, 5-6 weeks) were purchased from Beijing HFK Bioscience Co. Ltd, Beijing, China. All the animals used in the experiments were treated humanely in accordance with the Institutional Animal Care and Use Committee Guidelines of Jinan University.

Production of fully Humanized Monoclonal Antibodies

The CDR-grafted sequence was constructed by selecting fully human antibody VL and VH domains that had the highest sequence similarity with the murine antibody (E12) in NCBI BLAST. Each homologous human VL and VH domain of interest was substituted with E12 complementarity-determining regions (CDRs) to produce the CDR-grafted humanized variants (H1L1, H2L2 and H3L3). To obtain a stable structure, the energy of model was minimized using proprietary structural optimization software until the energy gradients reached the optimal level. Recombinant plasmids, containing the various optimized combinations of light and heavy chains, were transiently transfected into mammalian 293F cells(2×10⁶cells/ml) at a density of 0.5 mg/L and cultured for 5 days before the cultural supernatant was collected.

Immunofluorescence assay

bFGF and H3L3 were conjugated with PE and FITC, respectively. All steps were performed according to the product brochure. H460 cells were seeded in 6-well plates and incubated overnight at 37°C. The cells were washed with PBS three times prior to treatment with H3L3-FITC + bFGF-PE or bFGF-PE alone. After 1h of treatment the cells were imaged using laser scanning confocal microscopy.

Cell viability assay

The effects of H3L3 on cell viability were evaluated by CCK8 assay. H460 cells were seeded to 96-well plates at 3000 cells/well and incubated overnight at 37°C. After treating with 0.5% FBS in DMEM for 12 h, the experimental group was treated with serially diluted H3L3 plus 20 ng/mL bFGF for 72 h. The cells were then incubated with Cell Counting Kit-8 solution at 37°C for 3 h (CCK-8; Dojindo

Laboratories, Kumamoto, Japan) and detected at OD₄₅₀ in the ELISA reader (BioTek).

Wound healing assay

H460 cells were seeded in 6-well plates and incubated overnight at 37°C. When the cells had grown to confluence, a cell-free area was introduced in the monolayer using a pipette tip. The test and control groups received different treatments (H3L3: 200 µg/ml H3L3 + 20 ng/mL bFGF; Control: 20 ng/mL bFGF). The cells were captured for analysis at 0 h and 24 h.

Western blot assay

H460 cells were seeded in 6-well plates, treated with serially diluted H3L3 and 0.5% FBS with or without bFGF (20 ng/mL) and incubated for 48 h. Cells were lysed with RIPA lysis buffer at 4°C for 10 min (Beyotime Biotechnology, Suzhou, China). The lysates were transferred into new EP tubes and centrifuged at 12,000g for 10 min at 4°C. The Pierce BCA Protein Assay Kit (Thermo Scientific, Rockford, IL, USA) was used to quantify total protein. The proteins were separated by 12% SDS-PAGE and transferred to PVDF membrane (Millipore) and then blocked with 5% nonfat milk at 37°C for 1h, incubated with rabbit anti-t/p-MAPK (4695/4370; Cell Signaling Technology, Danvers, MA, USA) and rabbit anti-t/p-Akt (4691/4060; Cell Signaling Technology) at 4°C overnight. The membrane was then incubated with the HRP-conjugated goat anti-rabbit IgG for 1h at 37°C. The blots were detected with an Immobilon Western chemiluminescent HRP Substrate (Millipore) according to the manufacturer's protocol.

Transwell assay

HUVEC cells were transferred to inserts of each transwell chamber (BD Biosciences, Bedford, MA, USA) with CM of H460 cell cultures. H3L3 (200 µg/ml) and isotype IgG was added to the inserts and incubated at 37°C for 24 h. Controls received the medium with DMSO. The lower chambers contained 600 µL complete medium as a chemoattractant. After 24 h, the cells on the upper side of the filters were mechanically removed, and those that had migrated into the lower side were fixed with 75% ethanol (20 min), stained by 0.1% crystal violet (Meryer, Shanghai, China), and imaged with a computerized imaging system.

Tube formation assay

Matrigel matrix (50 µl/well) was added into 96-well plates. The plates were incubated for 30 min at 4°C and then for 30 min at 37°C. HUVEC (5×10⁴ cells/well) suspended in DMEM complete medium with 20 ng/mL bFGF were seeded to each well.

Purified H3L3 (200 µg/ml) and isotype antibody were added and incubated for 16 h. Tube formation was observed under a microscope and tube numbers were counted in five random high-power fields.

In vivo xenograft studies

H460 cells (5×10⁶) were subcutaneously injected into the back of BALB/c-nu mice. Once the tumors were palpable, the BALB/c-nu mice were randomly assigned into five treatment groups (five mice per group). H3L3 (25mg/kg, 12.5mg/kg, 6.25mg/kg), Cisplatin (2.5mg/kg), or PBS was injected into the tumors. All groups were injected six times at 3 day intervals. A vernier caliper was used to measure tumor size in two dimensions. Tumor volume (mm³) was calculated as $v=1/2(a \times b^2)$. a: length of tumor, b: width of tumor. The rate of tumor growth inhibition was calculated as $(1 - \frac{\text{mean of the tumor volume of treated groups}}{\text{mean of the tumor volume of PBS group}}) \times 100\%$.

Statistical analysis

Data are expressed as the mean and standard deviation (SD). P<0.05 were considered statistically significant. Assays were performed at least three times independently.

Results

Humanization of the murine antibody E12

The anti-bFGF murine antibody (E12) was selected as a template to construct the human monoclonal antibody. To achieve maximum humanization, we altered the constant and CDR regions to mimic that of its most similar aligned peptide from a human germline antibody producing three strains of humanized antibodies (Fig. 1A, B). After making all possible single substitutions to simulate the human germline sequence, the number of mutations produced less diversity among light chains compared to heavy chains, and the humanization of heavy and light chains in H1L1, H2L2 and H3L3 were 93.26, 82.22; 94.38, 92.22; and 100%, 98.89% respectively (Fig. 1E, F). In addition, we assessed the affinity of these antibodies by ELISA, and found that they all display favorable affinities and stabilities at high temperatures, have alkali resistance, and can withstand repeated freeze-thaw cycles (Supplementary Table S1, Fig. S1). Based on these analyses, we chose the humanized monoclonal antibody H3L3 for further investigation. In order to verify whether the spatial structure was changed after the antibody humanized, we compared the interactions of bFGF with E12 and H3L3 by homology modeling. The structural stability was evaluated by rotameric energy. Molecular docking analysis showed

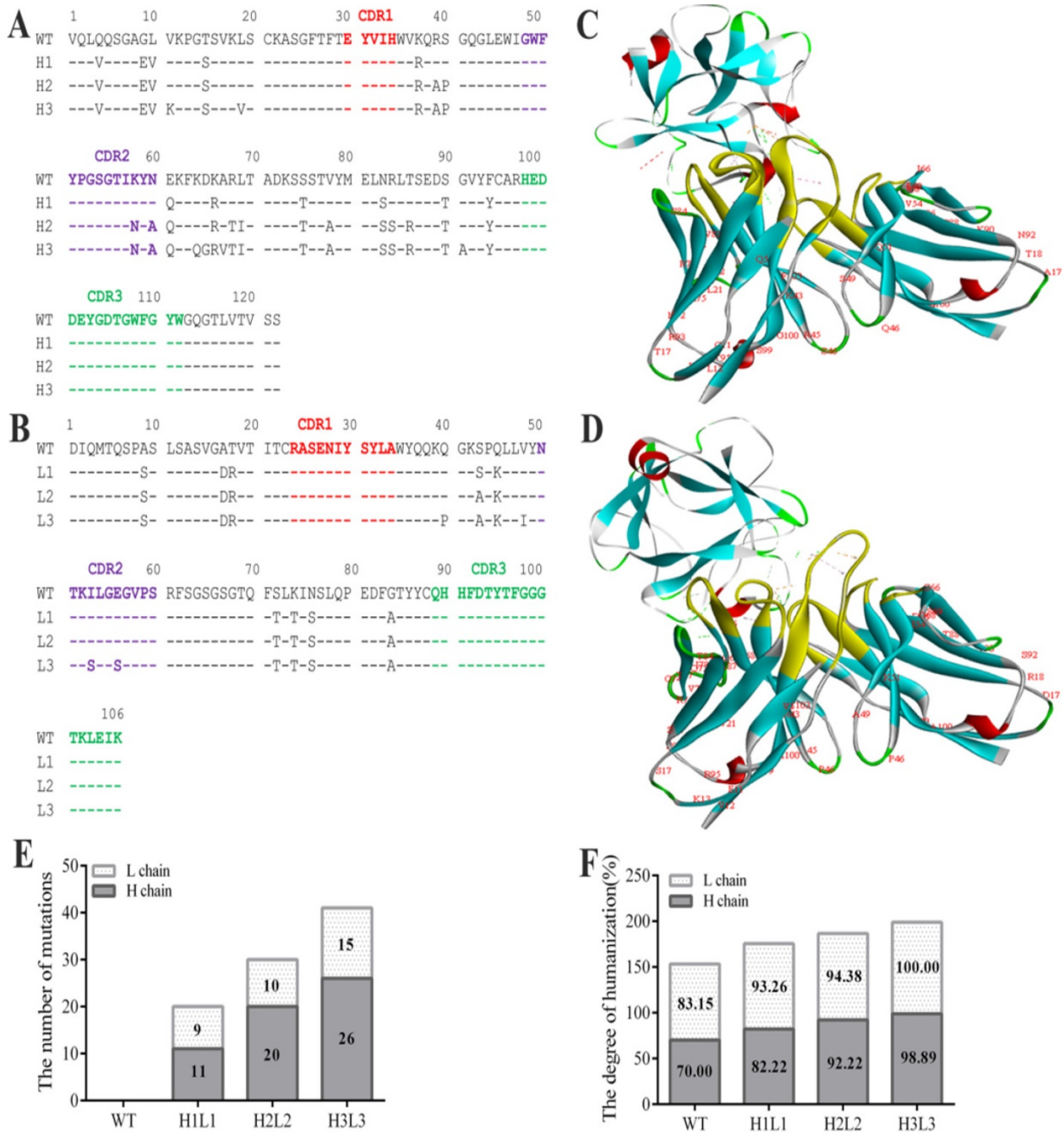


Figure 1. Sequence analysis the humanization of murine antibody. (A)CDR of heavy chain; (B) CDR of light chain; (C) Molecular docking of mouse monoclonal antibody(E12) and (D) humanized monoclonal antibody(H3L3) with bFGF. (E)The number of base substitutions in light chain (L chain) and heavy chain (H chain). (F) The degree of humanization among L chains and H chains in WT(E12), H1L1, H2L2 and H3L3. WT represents the murine monoclonal antibody; light chain(White); heavy chain(gray).

that the humanized CDR regions did not affect the binding of H3L3 to bFGF (Fig. 1C, D). These data indicate that H3L3 is stable and is theoretically able to bind bFGF.

H3L3 significantly inhibits the proliferation and migration of H460 cells, and migration and angiogenesis of HUVEC cells

After the identification and purification of H3L3 by reducing and non reducing SDS-PAGE and SEC-HPLC assays, we determined that the heavy and

light chains assembled into a complete antibody with a molecular weight of 150 KD (Supplementary Fig. S2). We further investigated its effect on the viability of H460 cells using the CCK8 kit. At 500 µg/ml of H3L3, the inhibition rate reached 66.82%, and this inhibitory capacity was dose-dependent in a certain range (Fig. 2A). In addition, the migration rate of H460 cells was markedly decreased to 60.00% compared to the control after 24h in wound healing assay (Fig. 2C, F). The migration of endothelial cells plays a key role in tumor angiogenesis[22]. Migration

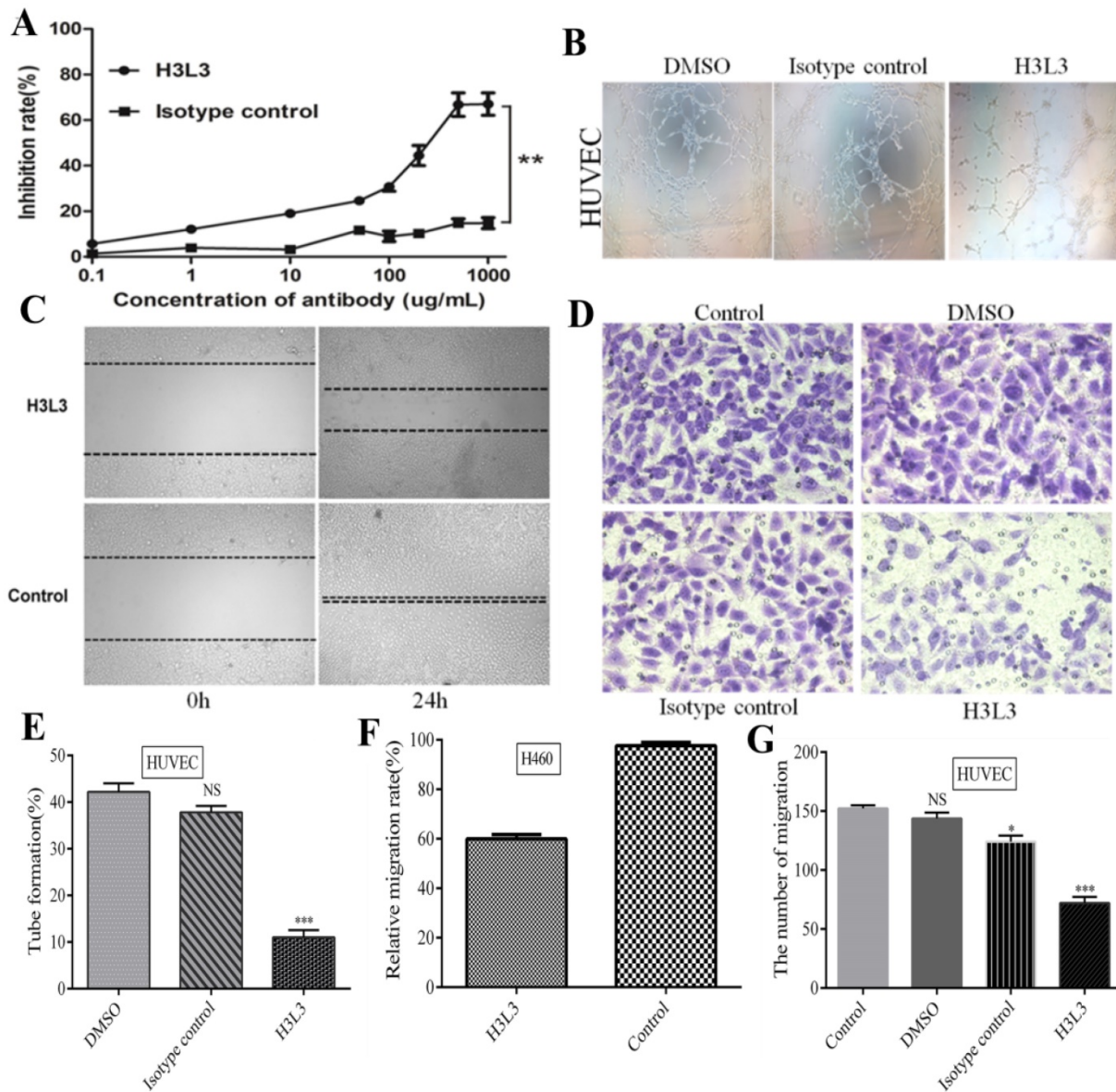


Figure 2. H3L3 effectively inhibited the proliferation, migration, angiogenesis of H460 and HUVEC cells. (A) The proliferation of H460 cells were assayed by CCK8-kit. (B) Tubules were sparser in H3L3 cultures compared to their corresponding control (0.01% DMSO) in HUVEC. (C) H3L3 suppresses the migration of H460 cells at 0h and 24h measured by a Wound healing assay (200 \times magnification). (H3L3: 200ug/ml H3L3 + 20ng/ml bFGF; Control: + 20ng/ml bFGF). (D) HUVEC were treated with the condition medium (CM) of H460 cell supernatant, adding with DMSO (0.01%), Isotype IgG and H3L3, respectively, complete by Boyden chamber assay. (E-G) Histograms represented the percentage of tube formation (E) and relative migration rate in the wound healing assay (F) numbers of migration of HUVEC cells in the Transwell assay (G). Data are presented as the mean \pm SD of three independent experiments performed in triplicate. NS: no significant; * $P < 0.05$, ** $P < 0.01$, *** $P < 0.001$.

of HUVEC cells was significantly reduced in the H3L3-treated group compared to the control in transwell assay (Fig. 2D, G). Tube formation rates in groups treated with DMSO, the isotype antibody control, and H3L3 were 42.2%, 37.8%, and 11.0%, respectively (Fig. 2B, E). These results demonstrate that H3L3 can effectively inhibit the proliferation and migration of H460 cells, and that it can also decrease the migration and angiogenesis of HUVEC cells.

H3L3 inhibits the proliferation of H460 cells via FGF2/FGFR signaling pathways

We next investigated the signaling pathways through which H3L3 influences cancer progression. It

has been reported that PI3K/AKT/mTOR and MAPK/ERK are the main signaling pathways that affect cancer cells proliferation [23]. Western blot revealed that H3L3 markedly inhibited the phosphorylation of MAPK and AKT in H460 cells in a dose-dependent manner (Fig. 3A). We then used immunofluorescence assays to explore whether H3L3 could block the binding of bFGF to extracellular FGFRs. The results implied that bFGF could effectively bind FGFRs and that H3L3 may inhibit the ability of bFGF to bind FGFRs on the cell surface, thereby preventing the activation of the downstream FGF2/FGFR signaling pathways (Fig. 3B).

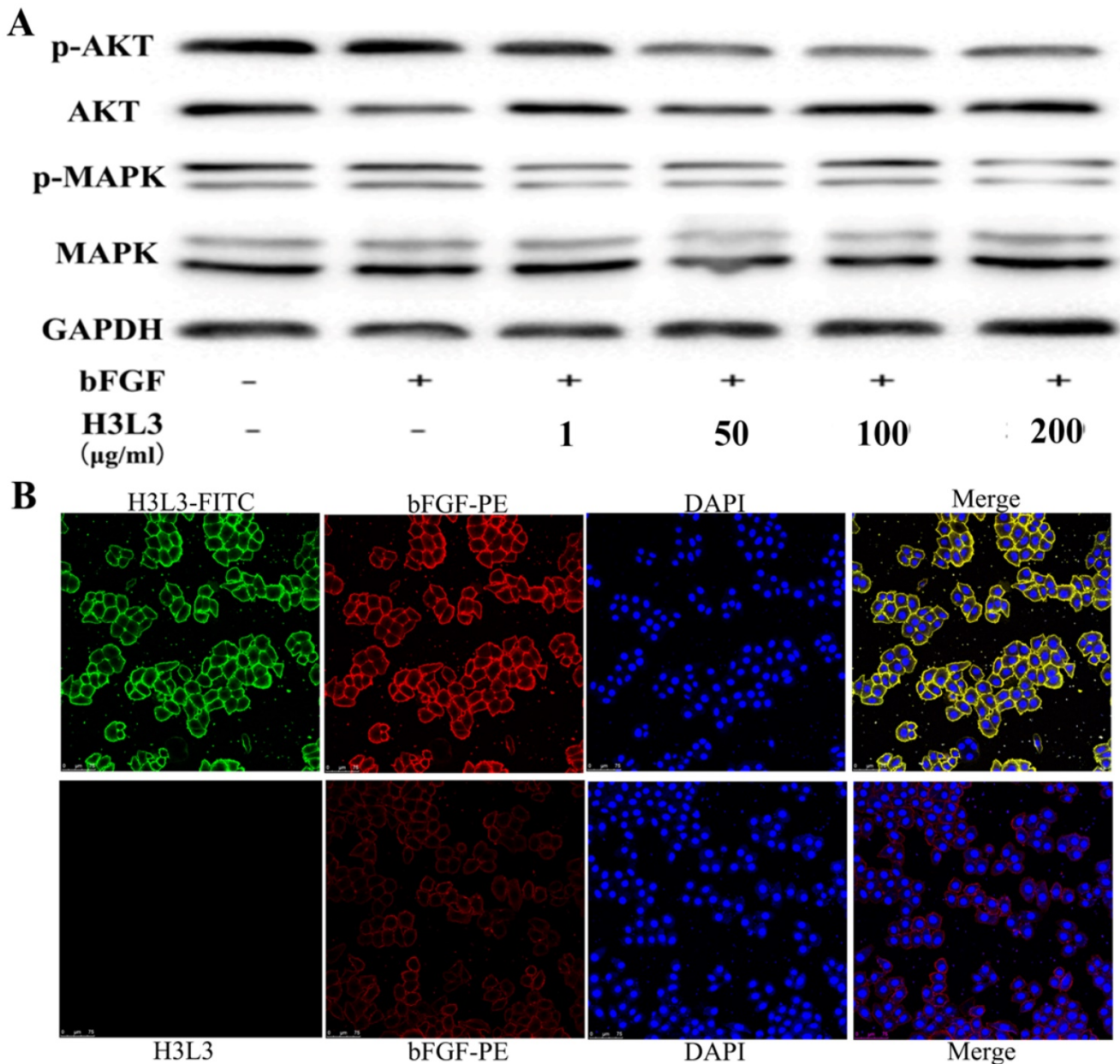


Figure 3. The mechanism and combined form of H3L3 in H460 cells. (A)H3L3 suppresses the proliferation of H460 cell by MAPK and AKT signaling pathways by Western blot assay. GAPDH was used as the reference control. (B) Immunofluorescence assay revealed the binding of H3L3 to bFGF and then interacted with FGFRs by using confocal microscope. The data showed as statistical analysis of the mean OD450 in various group, presented as the mean±SD of three independent experiments performed in triplicate.

H3L3 suppresses tumor growth in vivo

To investigate whether H3L3 exerts potent anti-tumor effects in vivo, we establish the tumor model via hypodermic injection of H460 cells in nude mice. Consistent with the results in vitro, H3L3 could markedly inhibit tumor growth in comparison with the control group(PBS) in a dose dependent manner (Fig. 4A). The tumor volumes were larger in the H3L3-treated group than Cisplatin-treated group. However, the tumor volume in the H3L3-treated group was significantly reduced compared to the control (Fig. 4B, C). Inhibition of tumor growth

reached 68.84% with H3L3 treatment (25 mg/mL) (Fig. 4D). To further investigate the side effects of H3L3 in nude mice, we measured the weight of BABL/c-nu mice every three days after injection of H3L3. We found the weight of BABL/c-nu mice was relatively stable (Fig. 4E). Moreover, H3L3 visibly reduced the formation of micro-vessel density in tumor xenografts (Fig. 4F, G). These results indicate that H3L3 is able to suppress tumor growth in vivo.

Taken together, our data indicate that the fully human monoclonal antibody (H3L3) could effectively suppress the progression or growth of NSCLC by targeting bFGF/FGFRs.

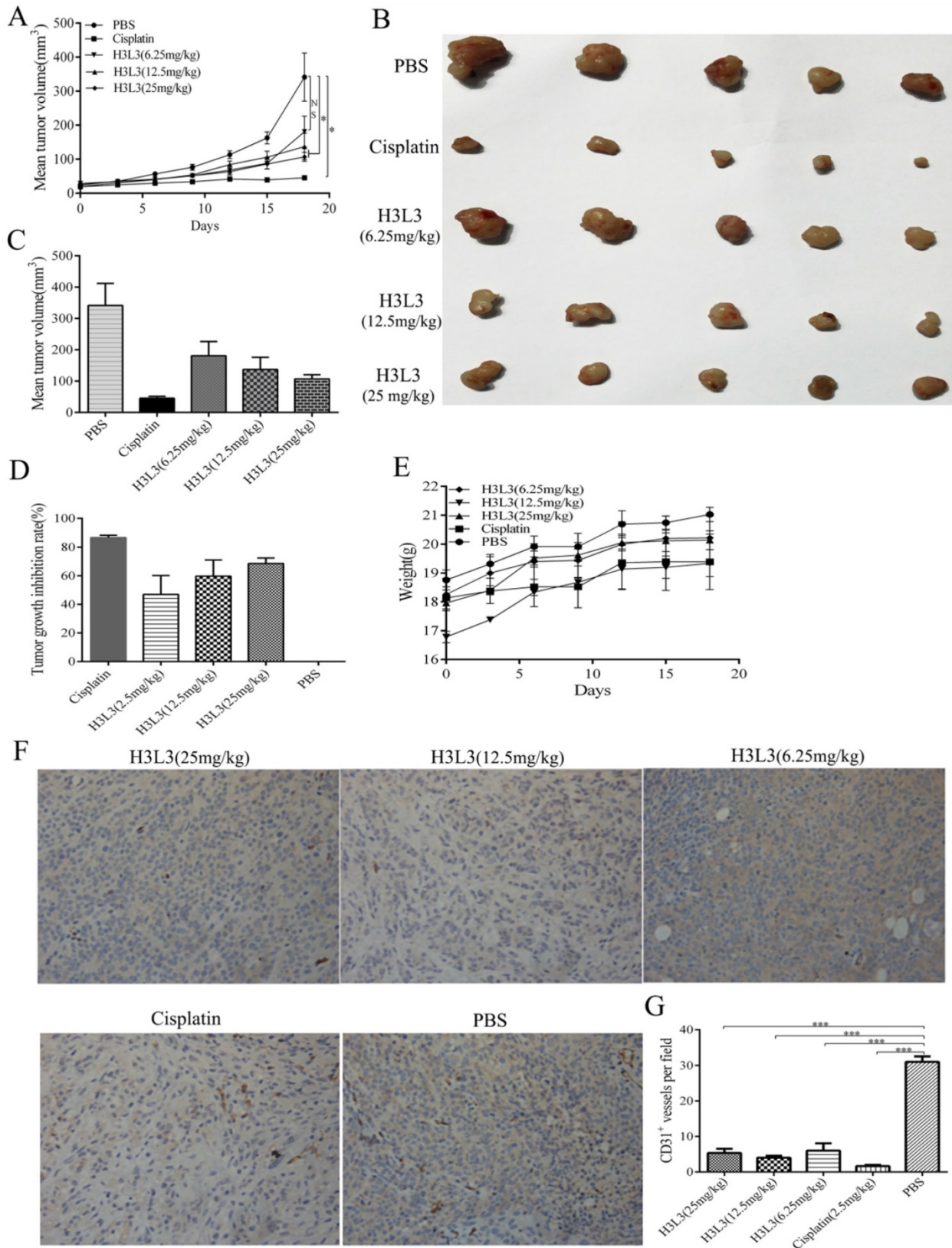


Figure 4. The inhibitory effects of H3L3 on the tumor growth in vivo. (A) Changes in tumor volume during the days of the experiment in different groups. (B) Photographs of xenograft tumors formed from H460 cells in different experiment groups. (C) Histogram showing the volume of different experiment groups. (D) Histogram revealing the inhibition rate of tumor growth in different experiment groups compared to control (PBS). Cisplatin is the positive group. (E) Weight of BABL/c-nu mice were measured every three days during the experiments in different groups. The data are presented as means \pm SD from five mice. (F) Tumor xenografts established from H460 cells are immunostained for CD31 and analysed for micro-vessel density, treated with H3L3(25mg/kg), H3L3(12.5mg/kg), H3L3(6.25mg/kg), Cisplatin(2.50mg/kg) and PBS, respectively. (G) Quantification of the micro- vessel density. Data are presented as the mean \pm SD of three independent experiments performed in triplicate. ***P<0.001.

Discussion

bFGF plays an important role in the growth, metastasis and angiogenesis of tumors including lung cancer, it is a valuable target of investigation[24-26]. Previously, we produced the murine anti-bFGF monoclonal antibody (E12), which could inhibit the metastasis of LLCs, but it existed the heterogeneous and would induce an HAMA response if used in humans. These limitations led us to modify the murine antibody, with the goal of humanizing it to prevent an unwanted immune response while maintaining its affinity and specificity for bFGF, and its stability. More importantly, humanization is widely applicable due to its well-developed technology and low cost. It occupies a large part of the monoclonal antibody market and has produced promising clinical candidates [27]. Antibodies can be humanized via resurfacing, framework shuffling, phage display approaches and specificity determining residue grafting[28]. Moreover, analysis of the crystal structures of antigen-antibody complexes shows that less than 33% of CDR residues are directly involved in antigen-antibody interactions and when CDR residues are changed, it can increase affinity for the antigen[29]. However, traditional CDR grafting by transplanting key antigen- recognizing residues from an exogenous antibody onto a human antibody generally produces a humanized antibody that has low immunogenicity or fails to express[30]. Thus, we have produced three strains of human full-length monoclonal antibodies based on E12 using structure-based computational protein design to simulate the crystal structure, which closely resembles the actual structure. Among them, H3L3 has the highest humanization and affinity, and a humanization percent for the heavy and light chains of 100% and 98.89%, respectively.

Multiple mechanisms have been described to explain how monoclonal antibodies exert their function on tumors. In general, bFGF and FGFRs dimerize leading to a conformational change and the formation of a tetrameric complex on the cell surface, which will activate the downstream signaling pathways. However, from Immunofluorescence and Western blot assays, we found that H3L3 could reduce the expression of p-AKT and p-MAPK in downstream signaling pathways, but could not completely block the binding of bFGF and FGFR1. The affinity of bFGF to FGFR1 is 1.2×10^{-10} [31], but H3L3 with FGFR1 is only 1×10^{-9} , which may be the main reason for the effect of H3L3. Our next step is to clearly define the CDR boundaries to increase the affinity of H3L3 by altering the residues in or around the CDR based on homology modeling.

Most tumors are sensitive to chemotherapy during the first round of treatment, but recurrent tumors often develop drug resistance, which is a major hurdle to successful therapies. Targeted therapy using humanized antibodies is beneficial for individualized and precise treatment of tumors. Angiogenesis is controlled by multiple signaling pathways, including bFGF and VEGF or PDGF, making treatment with single-target anti-vascular drugs impractical[32-34]. Treatments targeting multiple signaling pathways simultaneously have been and continue to be developed to face this challenge. In addition, by enabling the simultaneous engagement of two distinct targets, bispecific antibodies can broaden the potential utility of antibody-based therapies[35, 36]. Along these lines, application of H3L3 in combination with other drugs could provide personalized treatments. Combination therapy may be a promising and effective strategy to suppresses cancer progression by simultaneously acting on different targets, which could achieve better therapeutic outcomes for patients.

Collectively, our data demonstrate that the human full-length monoclonal antibody H3L3, with humanization of light and heavy chains of 100% and 98.89%, respectively, could bind to bFGF comparably to the murine monoclonal antibody E12. In addition, H3L3 could effectively suppress tumor progression *in vitro* and *in vivo*. H3L3 may be a promising antibody to block the progression of NSCLC.

Supplementary Material

Supplementary figures and tables.

<http://www.jcancer.org/v09p2003s1.pdf>

Acknowledgements

This study was funded by grants from the National Natural Science Foundation of China, No. 81202449; and Guangdong Province Key Scientific Research Grant, No. 2013A022100031.

Ethical approval

All applicable international, national and or institutional guidelines for the care and used of animals were followed.

Competing Interests

The authors have declared that no competing interest exists.

References

1. Cetin K, Ettinger DS, Hei YJ, O'Malley CD. Survival by histologic subtype in stage IV nonsmall cell lung cancer based on data from the Surveillance, Epidemiology and End Results Program. *Clinical epidemiology*. 2011; 3: 139-48.
2. Lin JM, Zhao JY, Zhuang QC, Hong ZF, Peng J. Xiongshao capsule promotes angiogenesis of HUVEC via enhancing cell proliferation and up-regulating the

- expression of bFGF and VEGF. Chinese journal of integrative medicine. 2011; 17: 840-6.
3. Sukmana I, Vermette P. The effects of co-culture with fibroblasts and angiogenic growth factors on microvascular maturation and multi-cellular lumen formation in HUVEC-oriented polymer fibre constructs. *Biomaterials*. 2010; 31: 5091-9.
 4. Boyd SR, Tan DS, de Souza L, Neale MH, Myatt NE, Alexander RA, et al. Uveal melanomas express vascular endothelial growth factor and basic fibroblast growth factor and support endothelial cell growth. *The British journal of ophthalmology*. 2002; 86: 440-7.
 5. Plotnikov AN, Schlessinger J, Hubbard SR, Mohammadi M. Structural basis for FGF receptor dimerization and activation. *Cell*. 1999; 98: 641-50.
 6. Eswarakumar VP, Lax I, Schlessinger J. Cellular signaling by fibroblast growth factor receptors. *Cytokine & growth factor reviews*. 2005; 16: 139-49.
 7. Turner N, Grose R. Fibroblast growth factor signalling: from development to cancer. *Nature reviews Cancer*. 2010; 10: 116-29.
 8. Akl MR, Nagpal P, Ayoub NM, Tai B, Prabhu SA, Capac CM, et al. Molecular and clinical significance of fibroblast growth factor 2 (FGF2 /bFGF) in malignancies of solid and hematological cancers for personalized therapies. *Oncotarget*. 2016; 7: 44735-62.
 9. Dirix LY, Vermeulen PB, Pawinski A, Prove A, Benoy I, De Pooter C, et al. Elevated levels of the angiogenic cytokines basic fibroblast growth factor and vascular endothelial growth factor in sera of cancer patients. *British journal of cancer*. 1997; 76: 238-43.
 10. Sezer O, Jakob C, Eucker J, Niemoller K, Gatz F, Wernecke K, et al. Serum levels of the angiogenic cytokines basic fibroblast growth factor (bFGF), vascular endothelial growth factor (VEGF) and hepatocyte growth factor (HGF) in multiple myeloma. *European journal of haematology*. 2001; 66: 83-8.
 11. Iwasaki A, Kuwahara M, Yoshinaga Y, Shirakusa T. Basic fibroblast growth factor (bFGF) and vascular endothelial growth factor (VEGF) levels, as prognostic indicators in NSCLC. *European journal of cardio-thoracic surgery : official journal of the European Association for Cardio-thoracic Surgery*. 2004; 25: 443-8.
 12. Bodner-Adler B, Mayerhofer K, Czerwenka K, Kimberger O, Koelbl H, Bodner K. The role of fibroblast growth factor 2 in patients with uterine smooth muscle tumors: an immunohistochemical study. *European journal of obstetrics, gynecology, and reproductive biology*. 2016; 207: 62-7.
 13. Cihoric N, Savic S, Schneider S, Ackermann I, Bichsel-Naef M, Schmid RA, et al. Prognostic role of FGFR1 amplification in early-stage non-small cell lung cancer. *British journal of cancer*. 2014; 110: 2914-22.
 14. Brown WS, Akhand SS, Wendt MK. FGFR signaling maintains a drug persistent cell population following epithelial-mesenchymal transition. *Oncotarget*. 2016; 7: 83424-36.
 15. Xiao XY, Lang XP. Correlation Between MMP-7 and bFGF Expressions in Non-small Cell Lung Cancer Tissue and Clinicopathologic Features. *Cell biochemistry and biophysics*. 2015; 73: 427-32.
 16. Bremnes RM, Camps C, Sireira R. Angiogenesis in non-small cell lung cancer: the prognostic impact of neoangiogenesis and the cytokines VEGF and bFGF in tumours and blood. *Lung cancer (Amsterdam, Netherlands)*. 2006; 51: 143-58.
 17. de Aguiar RB, Parise CB, Souza CR, Braggion C, Quintilio W, Moro AM, et al. Blocking FGF2 with a new specific monoclonal antibody impairs angiogenesis and experimental metastatic melanoma, suggesting a potential role in adjuvant settings. *Cancer letters*. 2016; 371: 151-60.
 18. Cai Y, Zhang J, Lao X, Jiang H, Yu Y, Deng Y, et al. Construction of a disulfide-stabilized diabody against fibroblast growth factor-2 and the inhibition activity in targeting breast cancer. *Cancer science*. 2016; 107: 1141-50.
 19. Pardo OE, Latigo J, Jeffery RE, Nye E, Poulosom R, Spencer-Dene B, et al. The fibroblast growth factor receptor inhibitor PD173074 blocks small cell lung cancer growth in vitro and in vivo. *Cancer research*. 2009; 69: 8645-51.
 20. Shkorporov AN, Khokhlova EV, Savochkin KA, Kafarskaia LI, Efimov BA. Production of biologically active scFv and VHH antibody fragments in *Bifidobacterium longum*. *FEMS microbiology letters*. 2015; 362: fmv083.
 21. Yang Y, Luo Z, Qin Y, Zhou Y, Gong L, Huang J, et al. Production of bFGF monoclonal antibody and its inhibition of metastasis in Lewis lung carcinoma. *Mol Med Rep*. 2017; 16: 4015-21.
 22. Zhang L, Huo X, Liao Y, Yang F, Gao L, Cao L. Zeylenone, a naturally occurring cyclohexene oxide, inhibits proliferation and induces apoptosis in cervical carcinoma cells via PI3K/AKT/mTOR and MAPK/ERK pathways. *Scientific reports*. 2017; 7: 1669.
 23. Nakashio A, Fujita N, Tsuruo T. Topotecan inhibits VEGF- and bFGF-induced vascular endothelial cell migration via downregulation of the PI3K-Akt signaling pathway. *International journal of cancer*. 2002; 98: 36-41.
 24. Yu M, Li SY, Yu Z, Qiu XS, Hou P, Wang EH, et al. [Clinical significance of heparanase and basic fibroblast growth factor expression in human non-small cell lung cancer]. *Zhonghua bing li xue za zhi = Chinese journal of pathology*. 2005; 34: 36-41.
 25. Kuhn H, Kopff C, Konrad J, Riedel A, Gessner C, Wirtz H. Influence of basic fibroblast growth factor on the proliferation of non-small cell lung cancer cell lines. *Lung cancer (Amsterdam, Netherlands)*. 2004; 44: 167-74.
 26. Formisano L, Jansen VM, Marciano R, Bianco R. From biology to therapy: Improvements of therapeutic options in Lung cancer. *Anti-cancer agents in medicinal chemistry*. 2017.
 27. Greulich H, Pollock PM. Targeting mutant fibroblast growth factor receptors in cancer. *Trends in molecular medicine*. 2011; 17: 283-92.
 28. Burnett MJ, Karki S, Moore GL, Leung IW, Chen H, Pong E, et al. Engineering fully human monoclonal antibodies from murine variable regions. *Journal of molecular biology*. 2010; 396: 1474-90.
 29. Almagro JC. Identification of differences in the specificity-determining residues of antibodies that recognize antigens of different size: implications for the rational design of antibody repertoires. *Journal of molecular recognition : JMR*. 2004; 17: 132-43.
 30. Zhang T, Wu MR, Sentman CL. An NKp30-based chimeric antigen receptor promotes T cell effector functions and antitumor efficacy in vivo. *Journal of immunology (Baltimore, Md : 1950)*. 2012; 189: 2290-9.
 31. Takayama S, Murakami S, Nozaki T, Ikezawa K, Miki Y, Asano T, et al. Expression of receptors for basic fibroblast growth factor on human periodontal ligament cells. *Journal of periodontal research*. 1998; 33: 315-22.
 32. Hu PH, Pan LH, Wong PT, Chen WH, Yang YQ, Wang H, et al. (125)I-labeled anti-bFGF monoclonal antibody inhibits growth of hepatocellular carcinoma. *World journal of gastroenterology*. 2016; 22: 5033-41.
 33. Ramjiawan RR, Griffioen AW, Duda DG. Anti-angiogenesis for cancer revisited: Is there a role for combinations with immunotherapy? *Angiogenesis*. 2017; 20: 185-204.
 34. Wang Z, Dabrosin C, Yin X, Fuster MM, Arreola A, Rathmell WK, et al. Broad targeting of angiogenesis for cancer prevention and therapy. *Semin Cancer Biol*. 2015; 35 Suppl: S224-s43.
 35. Spiess C, Merchant M, Huang A, Zheng Z, Yang NY, Peng J, et al. Bispecific antibodies with natural architecture produced by co-culture of bacteria expressing two distinct half-antibodies. *Nature biotechnology*. 2013; 31: 753-8.
 36. Yu YJ, Zhang Y, Kenrick M, Hoyte K, Luk W, Lu Y, et al. Boosting brain uptake of a therapeutic antibody by reducing its affinity for a transcytosis target. *Science translational medicine*. 2011; 3: 84ra44.